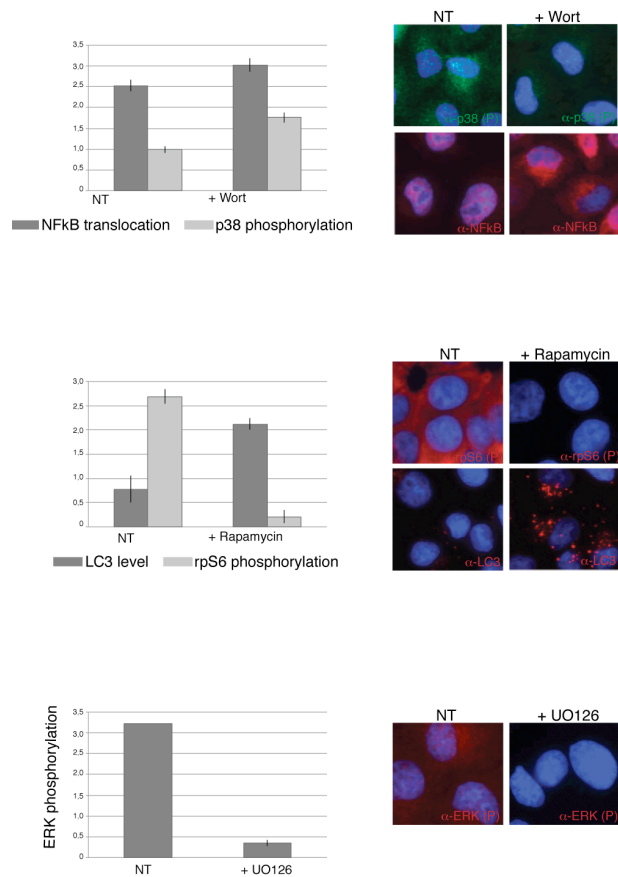


## ▪ **Supplementary Information**

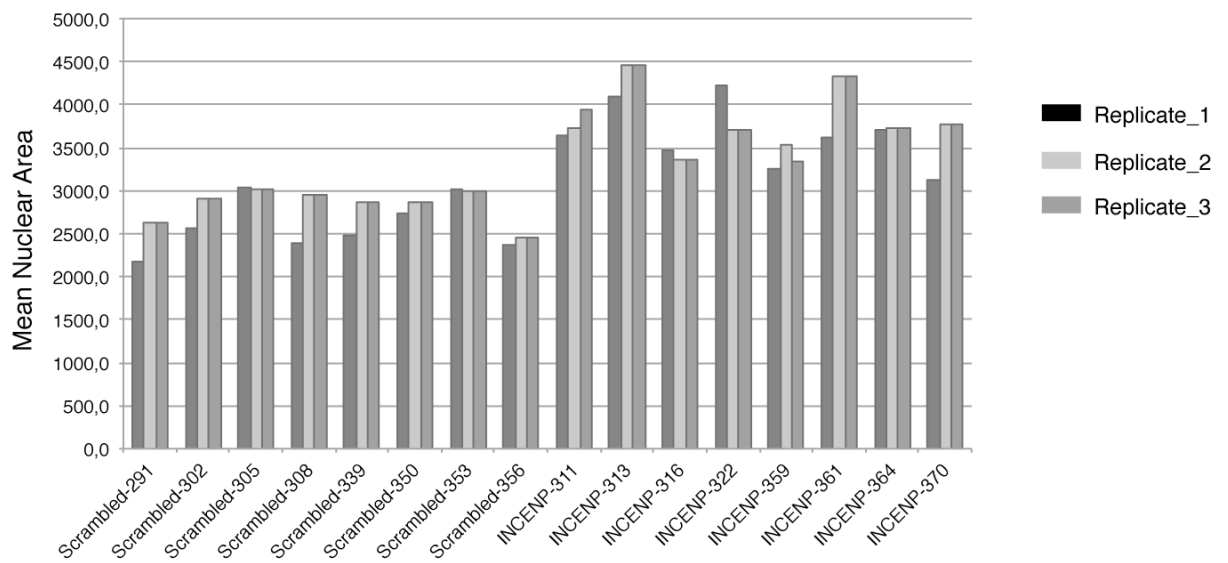
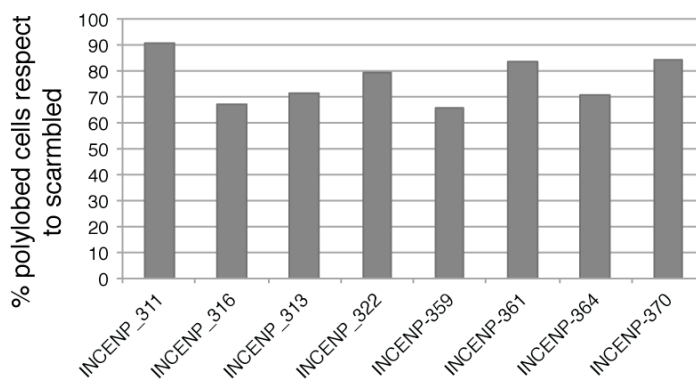
### **Table of contents**

- Fig. S1. Inhibition of specific upstream kinases affects the activity of the analyzed readouts
- Fig. S2. Down-regulation of INCENP gene induces the formation of polylobed nuclei.
- Fig. S3. Knock-down analysis of specific phosphatase mRNA by siRNA.
- Fig. S4. Hill normalization of experimental data.
- Fig. S5. Training of the HeLa Boolean model.
- Fig. S6. Performance of the optimized model.
- Table S1. siRNA screening results per cell (separate file)
- Table S2. siRNA primary screening results (separate file).
- Table S3. siRNA secondary screening results.
- Table S4. Literature-derived directed network.
- Table S5. Literature reported phosphatase-pathway relationship.
- Reference



**Fig. S1. Inhibition of specific upstream kinases affects the activity of the analyzed readouts.**

The NFkB and p38 activity was monitored in HeLa cells treated with 200  $\mu$ M wortamannin (PI3K inhibitor) per 2 hours and then stimulated with TNF $\alpha$  for 10 minutes. The mTOR as well as autophagy activation were analyzed in HeLa cells incubated with medium containing 100  $\mu$ M rapamycin (mTOR inhibitor) per 1 hour. While the ERK phosphorylation level was measured in cells treated with 10  $\mu$ M UO126 (MEK inhibitor) per 1 hour. Cells were fixed and stained with anti-phospho p38, anti-NFkB (p65), anti-LC3, anti-phospho rpS6 and anti-phospho ERK antibodies. Four images per samples were acquired by indirect immunofluorescence on Delta Vision microscope with a 20X objective. Images were automatically analyzed by Cell Profiler and the signal intensity of each antibody was measured in both the nuclear and the cytosolic compartments. NFkB activation was measured as the ratio between the nuclear and the cytosolic fraction in each cell. For each sample, the mean value was measured and plotted in the bar graph. ERK as well as p38 activation were measured as the phosphorylation level of such antibodies in the nuclear region. For each image, the mean values and standard deviation were measured and plotted in the bar graph. rpS6 phosphorylation as well as LC3 intensity were measured in the cytosolic region. For each image, the mean value and the standard deviation were calculated and plotted in the bar graph.

**A****B**

**Fig. S2. Down-regulation of INCENP gene induces the formation of polylobed nuclei. A)** Each LabTek, used in the primary screening, contains 8 control spots, in which the siRNA oligo targeting the INCENP gene was spotted. As previously demonstrated, the down-regulation of the INCENP gene induces the formation of polylobed nuclei<sup>1</sup>. To assess the transfection efficiency variability across the different spots of the different labTeks, the area of the nuclei was measured and plotted as bar graph. The three biological replicas are shown as different grey tones. **B)** The percentage of polylobed nuclei has been measured and plotted by counting the nuclei, whose area is larger than twice the mean nuclear area in scrambled controls. For a few images we have checked that this estimates match the frequency of polylobed cells as estimated visually.

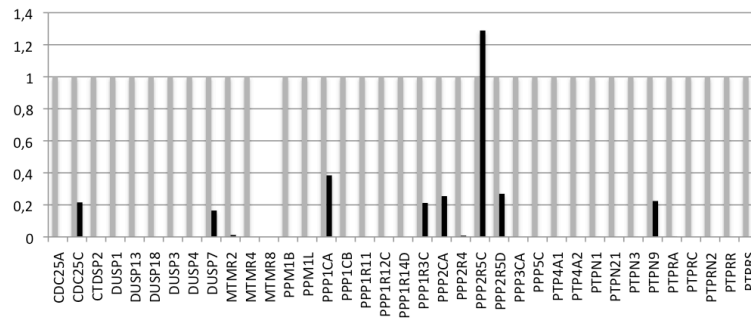


**Fig. S3. Knock-down analysis of specific phosphatase mRNA by siRNA.** Total RNA was isolated from HeLa cells and primers designed to specifically amplify the indicated phosphatases and a reference gene (HPRT) were used in RT-PCR reactions. Data were quantified and the relative mRNA expression was calculated applying the comparative CT method <sup>2</sup> and then plotted. mRNA levels were measured after introduction of three different siRNA oligos (black bar) or of a scrambled sequence, as negative control (grey bars).

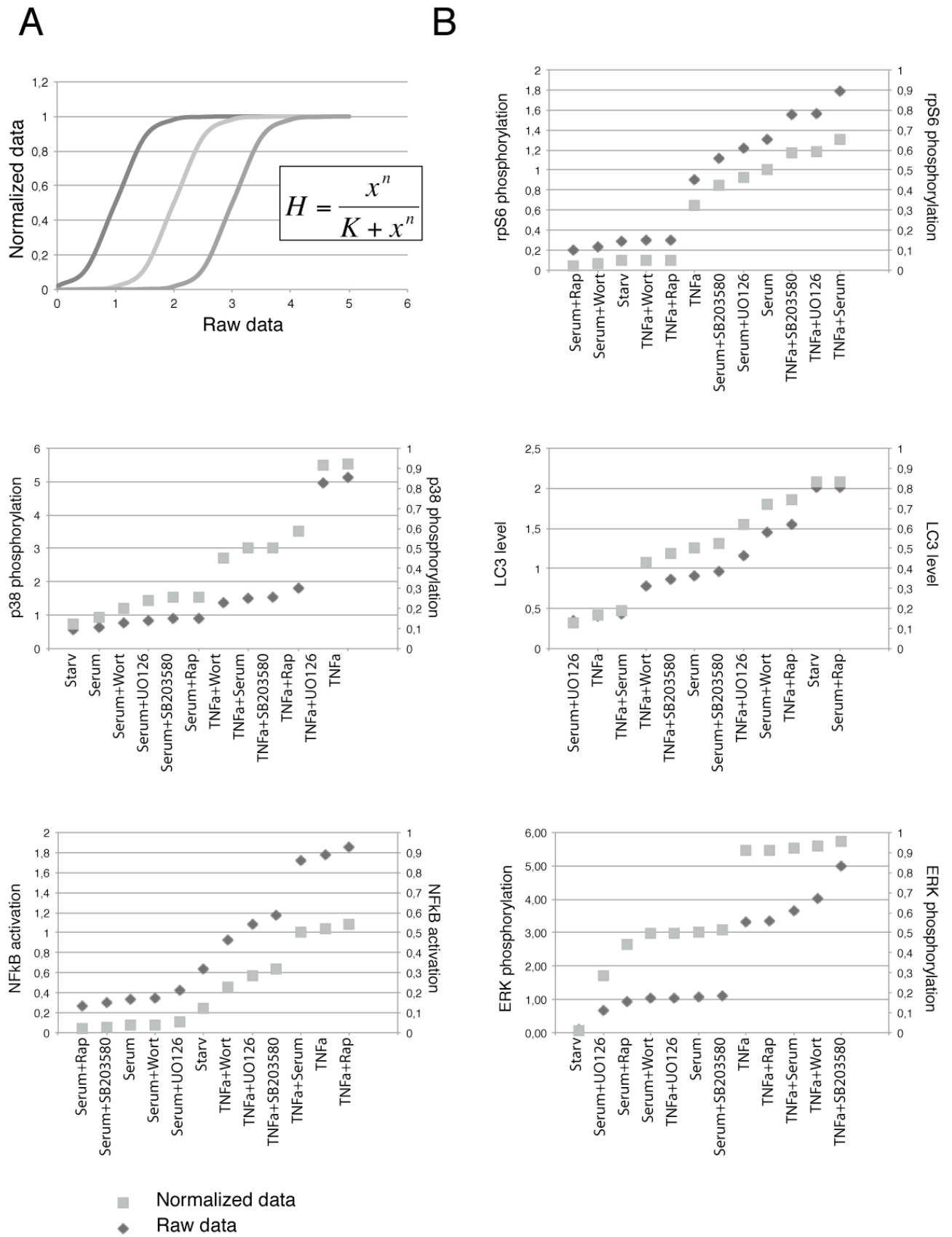
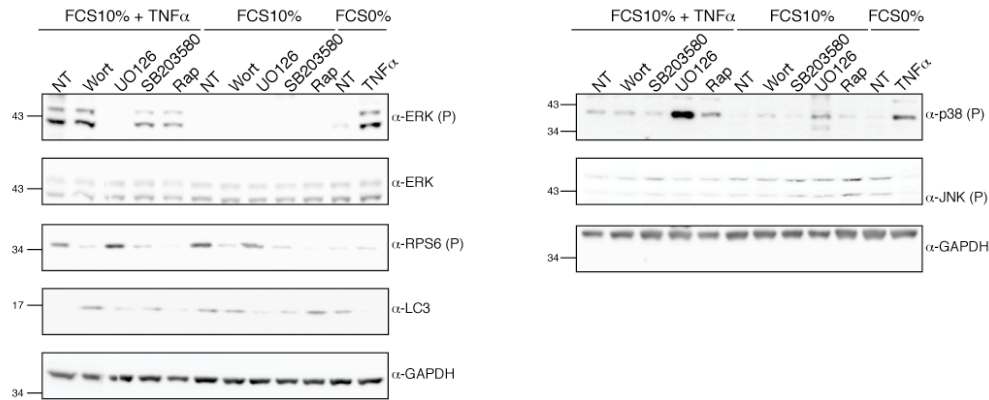


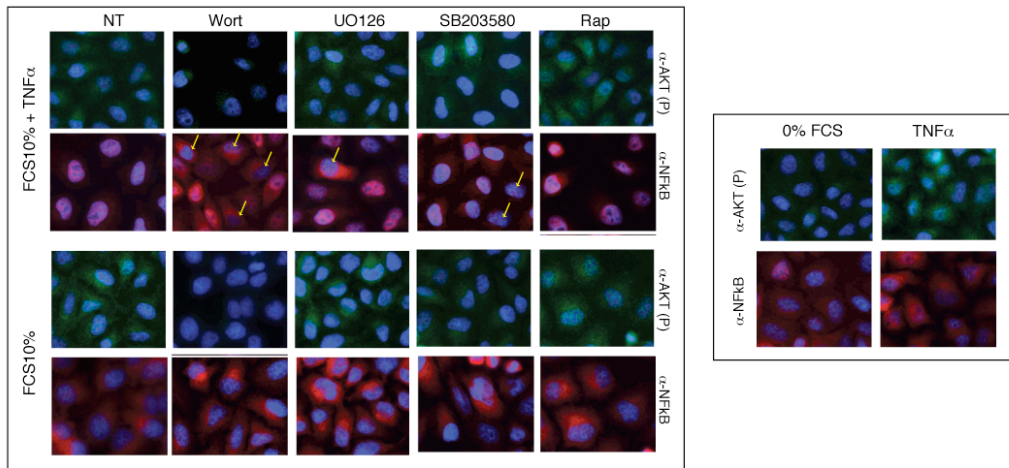
**Fig. S4. Hill normalization of experimental data.** A) Experimental data were normalized in the 0-1 range by the Hill function. Three different Hill functions have been plotted in the upper left panel. From left to right, the Hill functions have an inflection point at 1, 2, 3 respectively. For

each function, the Hill coefficient  $K$  was set to 2. **B to F**) For each analyzed phenotype, each measurement was normalized in the 0-1 range, by applying the Hill function. Dark grey points represent raw data, while light grey points represent normalized data. The different left and right y-scales represent raw and normalized values respectively. The points were sorted by raw value.

**A**



**B**



**C**

	ERK	LC3	RPS6	NFkB	p38	JNK	AKT	ERK	LC3	RPS6	NFkB	p38	JNK	AKT
TNF $\alpha$ +Serum	3.66	0.44	1.79	1.72	1.51	1.16	1.48	0.69	0.05	1.00	0.91	0.74	0.09	0.60
TNF $\alpha$ +Wort	4.01	0.79	0.30	0.93	1.36	1.06	0.30	0.77	0.26	0.06	0.42	0.70	0.01	0.00
TNF $\alpha$ +UO126	1.05	1.16	1.57	1.08	4.95	1.34	1.34	0.09	0.49	0.86	0.51	1.00	0.25	0.53
TNF $\alpha$ +SB203580	4.99	0.87	1.56	1.18	1.52	1.05	1.46	1.00	0.31	0.86	0.57	0.75	0.00	0.59
TNF $\alpha$ +Rap	3.34	1.54	0.30	1.86	1.79	1.14	2.12	0.62	0.72	0.07	1.00	0.80	0.08	0.92
Serum	1.05	0.91	1.30	0.34	0.64	1.07	2.09	0.09	0.34	0.70	0.04	0.17	0.01	0.91
Serum+Wort	1.04	1.45	0.23	0.35	0.76	1.11	0.50	0.09	0.66	0.02	0.05	0.33	0.05	0.10
Serum+UO126	0.66	0.35	1.22	0.42	0.85	1.27	2.08	0.00	0.00	0.64	0.10	0.42	0.20	0.90
Serum+SB203580	1.09	0.96	1.12	0.30	0.89	1.16	1.86	0.10	0.36	0.58	0.02	0.46	0.10	0.79
Serum+Rap	0.94	2.01	0.19	0.27	0.89	1.91	2.27	0.06	1.00	0.00	0.00	0.46	0.76	1.00
Starv	1.12	2.01	0.29	0.64	0.56	2.19	0.84	0.11	1.00	0.06	0.23	0.10	1.00	0.28
TNF $\alpha$	3.31	0.41	0.90	1.78	5.14	1.30	2.14	0.61	0.03	0.44	0.95	1.00	0.22	0.93

**Fig. S5. Training of the HeLa Boolean model.** HeLa cells treated, as indicated, were analyzed by SDS-PAGE or by Immuno-fluorescence. **A)** Protein extracts were revealed with anti-phospho ERK, anti-ERK, anti-LC3, anti-phospho rpS6, anti-phospho JNK, anti-phospho p38, anti-Tubulin and anti-GAPDH antibodies. **B)** Cells were fixed and stained with anti-NFkB (TRITC), anti-phospho AKT (FITC) and DAPI, to visualize nuclei. Four fields containing approximately

400 cells were acquired for each sample by indirect immunofluorescence (20X objective) and automatically analyzed by the Cell Profiler software. C) Intracellular signaling protein activity was quantified (raw data) and then, normalized by the Hill function, as described in Material and Method section. The red or green box color indicates respectively low and high values.



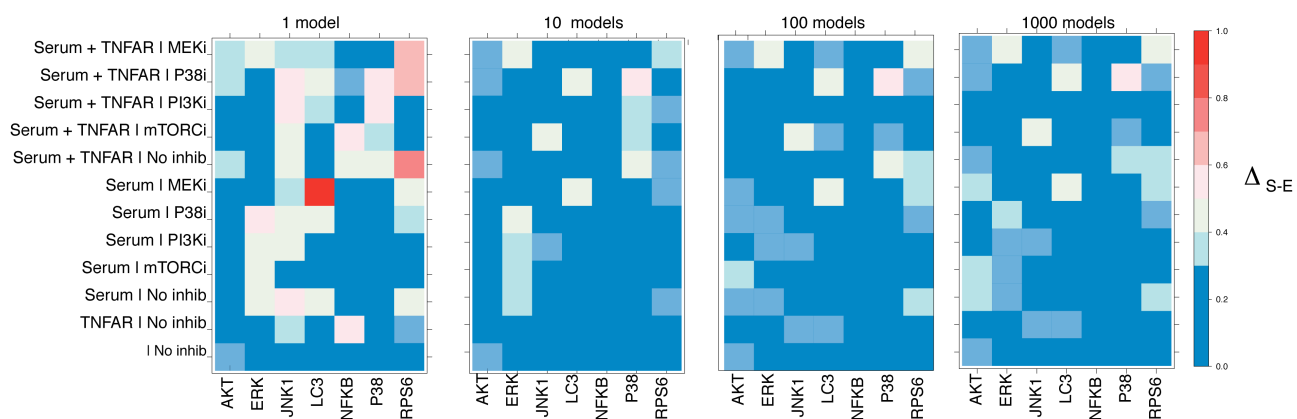


**Fig. S6. Performance of the optimized model.** The absolute value of the difference ( $\Delta$ ) between the model simulation results (S) to normalized experimental data (E), is represented with a color code. If  $\Delta_{S-E}=1$  (strongest disagree) or  $\Delta_{S-E}=0$  (strongest agree) the box color is red or blue respectively. Intermediate values of  $\Delta_{S-E}$  are mapped to shades of red and blue. Simulation results of the average of respectively 1, 10, 100, 1000 models are shown.

## ▪ **Supplementary Tables**

**Table S1. siRNA screening results per cell.** For each analyzed image, the mean intensity value of each cell has been reported.

See Supplementary Table S1.

**Table S2. siRNA primary screening results.** HeLa cells were transfected with three different oligos targeting 300 human phosphatases or phosphatase related genes and 84 positive (transfection control) and negative control oligos. For each phosphatase interfered by siRNA screening, Uniprot ID, gene name, protein name and Ambion Oligo ID have been reported. In addition according to substrate specificity, phosphatases were classified as Protein Tyrosine Phosphatase (PTP), Phosphoserine Proteine Phosphatases (PPP), Protein Phosphatase Metal dependent (PPM), Carboxy Terminal Domain phosphatases (CTD), Regulatory Subunits (RS), Sugar Phosphatase (SP), Lipid Phosphatase (LP), Nucleotide Phosphatase (NP) and Alkaline Phosphatase (ALP). As final value for each data point, the median of the three biological replicates was used. For each analyzed phenotype, a robust Z-score was calculated and reported (from column F to G).

See Supplementary Table S2.

Accession	Entry name	Phenotype	Readout ratio with respect to the scrambled control	Fraction of mRNA expression levels after interferencel	Validated
P30304	CDC25A	p38 phosphorylation	0,67	0,00	No
P30307	CDC25C	rpS6 phosphorylation	1,89	0,22	Yes
P30307	CDC25C	ERK phosphorylation	1,82	0,22	Yes
P30307	CDC25C	NFkB translocation	1,74	0,22	Yes
O14595	CTDSP2	ERK phosphorylation	1,19	0,00	No
O14595	CTDSP2	p38 phosphorylation	0,96	0,00	No
P28562	DUSP1	LC3-II level	1,73	0,00	Yes
P28562	DUSP1	rpS6 phosphorylation	0,41	0,00	Yes
Q9UI16	DUSP13	rpS6 phosphorylation	0,65	0,00	No
Q8NEJ0	DUSP18	rpS6 phosphorylation	2,18	0,00	Yes
Q8NEJ0	DUSP18	ERK phosphorylation	1,77	0,00	Yes
P51452	DUSP3	NFkB translocation	1,98	0,00	Yes
P51452	DUSP3	rpS6 phosphorylation	1,00	0,00	No
Q13115	DUSP4	rpS6 phosphorylation	0,49	0,00	Yes
Q13115	DUSP4	p38 phosphorylation	0,78	0,00	No
Q13115	DUSP4	NFkB translocation	0,49	0,00	Yes
Q16829	DUSP7	rpS6 phosphorylation	0,48	0,16	Yes
Q16829	DUSP7	p38 phosphorylation	1,44	0,16	Yes
Q13614	MTMR2	rpS6 phosphorylation	1,01	0,01	No
Q13614	MTMR2	ERK phosphorylation	1,55	0,01	Yes
Q9NYA4	MTMR4	LC3-II level	1,65	0,00	Yes
Q96EF0	MTMR8	ERK phosphorylation	1,04	0,00	No
O75688	PPM1B	rpS6 phosphorylation	0,98	0,00	No
O75688	PPM1B	NFkB translocation	1,64	0,00	Yes
Q5SGD2	PPM1L	LC3-II level	1,55	0,00	Yes
Q5SGD2	PPM1L	NFkB translocation	1,25	0,00	No
P62136	PPP1CA	rpS6 phosphorylation	1,89	0,38	Yes
P62140	PPP1CB	rpS6 phosphorylation	1,54	0,00	Yes
O60927	PPP1R11	LC3-II level	1,85	0,00	Yes
O60927	PPP1R11	ERK phosphorylation	2,18	0,00	Yes
Q9BZL4	PPP1R12C	LC3-II level	1,14	0,00	No
Q9BZL4	PPP1R12C	rpS6 phosphorylation	0,67	0,00	No
Q9NXH3	PPP1R14D	rpS6 phosphorylation	1,67	0,00	Yes
Q9NXH3	PPP1R14D	p38 phosphorylation	2,02	0,00	Yes
Q9NXH3	PPP1R14D	NFkB translocation	1,62	0,00	Yes
Q9UQK1	PPP1R3C	LC3-II level	1,57	0,21	Yes
Q9UQK1	PPP1R3C	rpS6 phosphorylation	0,39	0,21	Yes
P67775	PPP2CA	rpS6 phosphorylation	2,03	0,25	Yes
P30154	PPP2R1B	rpS6 phosphorylation	0,44	NA	Yes
Q15257	PPP2R4	ERK phosphorylation	1,93	0,01	Yes
Q13362	PPP2R5C	rpS6 phosphorylation	1,36	1,29	No
Q13362	PPP2R5C	ERK phosphorylation	1,23	1,29	No
Q14738	PPP2R5D	rpS6 phosphorylation	1,07	0,27	No
Q08209	PPP3CA	LC3-II level	2,02	0,00	Yes
Q08209	PPP3CA	ERK phosphorylation	1,85	0,00	Yes
Q08209	PPP3CA	rpS6 phosphorylation	1,79	0,00	Yes
P53041	PPP5C	LC3-II level	0,33	0,00	Yes
Q93096	PTP4A1	NFkB translocation	1,76	0,00	Yes
Q12974	PTP4A2	p38 phosphorylation	1,79	0,00	Yes
P18031	PTPN1	rpS6 phosphorylation	1,89	0,00	Yes
Q16825	PTPN21	LC3-II level	0,39	0,00	Yes
Q16825	PTPN21	ERK phosphorylation	0,35	0,00	Yes
Q16825	PTPN21	p38 phosphorylation	0,50	0,00	Yes
Q16825	PTPN21	NFkB translocation	0,49	0,00	Yes
P26045	PTPN3	rpS6 phosphorylation	1,54	0,00	Yes
P43378	PTPN9	rpS6 phosphorylation	1,79	0,22	Yes
P18433	PTPRA	p38 phosphorylation	1,80	0,00	Yes
P18433	PTPRA	NFkB translocation	1,67	0,00	Yes
P08575	PTPRC	LC3-II level	1,96	0,00	Yes
Q92932	PTPRN2	p38 phosphorylation	1,81	0,00	Yes
Q15256	PTPRR	LC3-II level	2,00	0,00	Yes
Q13332	PTPRS	rpS6 phosphorylation	1,84	0,00	Yes

**Table S3. siRNA secondary screening results.** HeLa cells were transfected with a pool of three plasmids (Mission<sup>®</sup> shRNA phosphatase library, Sigma) directing the synthesis of three different siRNA targeting each phosphatase hit and scrambled sequences. 48 hours after transfection, the cell cultures were stimulated with TNF $\alpha$  for 10 minutes or left untreated, as in the primary

screening. Upon phosphatase down-regulation, the activation level of ERK, p38 as well as autophagy was monitored by western-blot, whereas rpS6 phosphorylation and NFkB nuclear translocation were analyzed by indirect immunofluorescence. For each phosphatase hits, Uniprot ID and gene name have been reported in the first two columns. The phenotype affected by phosphatase interference is reported in the third column. Results are expressed as ratios with respect to the scrambled control (fourth column). Hits having a ratio lower than 0.5 or higher than 1.5 were classified as confirmed. The success in gene down regulation was monitored by quantitative PCR. The ratio of mRNA levels after and before shRNA treatment is reported in the fifth column. The final result of secondary screening is summarized in last column.

Uniprot A	Protein A	Effect	Uniprot B	Protein B	Pmid
P31749	AKT	-1	P04049	RAF	11443134
P31749	AKT	1	O14920	IKK	11259436
P31749	AKT	-1	Q92574	TSC	16636147
Q9C0C7	AMBRA1	1	Q14457	BCN1	17589504
Q9Y478	AMPK	1	Q92574	TSC	14651849/19584320
Q9Y478	AMPK	1	O75385	ULK	21205641/19584320
P10415	BCL2	-1	Q14457	BCN1	18570871
Q14457	BCN1	1	Q92574/Q9C0C7/Q9B	LC3	18843052
P53355	DAPK	1	Q14457	BCN1	19180116
P53355	DAPK	1	P28482	ERK	15616583
P28482	ERK	1	O75582	MSK	15568999/9687510/18267068
P28482	ERK	-1	Q16539	P38	11842088/18481201
P28482	ERK	-1	P01112	RAS	8626428
P28482	ERK	-1	Q92574	TSC	17671177
P28482	ERK	1	P53355	DAPK	15616583
O14920	IKK	1	Q04206	NFKB	9346241/18267068
O14920	IKK	1	Q16539	P38	11259436/18267068
P45983	JNK1	-1	P10415	BCL2	18570871
Q02750	MEK	1	P28482	ERK	9677429
Q02750	MEK	1	P28482	ERK	9677429
O75582	MSK	1	Q04206	NFKB	12628924/18267068
P42345	mTORC	1	Q15418	S6K	15809305
P42345	mTORC	1	O75385	ULK	19690328
Q16539	P38	1	O75582	MSK	15568999/ 9687510/18267068
Q16539	P38	-1	P28482	ERK	18481201
P42336	PI3K	1	P31749	AKT	12167717
P01112	RAS	1	P04049	RAF	8622647
Q15418	S6K	1	P62753	RPS6	15809305
Q15418	S6K	-1	P45983	JNK1	17181399
na	Serum	-1	P45983	JNK1	15899879
na	Serum	-1	Q9Y478	AMPK	19584320
P19438	TNFR	1	Q16539	P38	16813528
P19438	TNFR	1	O14920	IKK	10795740
P19438	TNFR	1	P45983	JNK1	15837794
Q92574	TSC	-1	P42345	mTORC	12271141
O75385	ULK	1	Q9C0C7	AMBRA1	20921139
P01112	RAS	1	P42336	PI3K	8052307
P19438	TNFR	1	P62993	GRB2	10359574
P62993	GRB2	1	Q07889	SOS	8479541
Q07889	SOS	1	P01112	RAS	8493579
P62993	GRB2	1	Q13480	GAB1	12766170
Q13480	GAB1	1	P42336	PI3K	11606067
P04049	RAF	1	Q02750	MEK	8621729
na	Serum	1	P62993	GRB2	9356464
P42345	mTORC	1	O14920	IKK	18519641
P19438	TNFR	1	O43318	TAK1	16260783
O43318	TAK1	1	P45985	MKK4	17875933
P45985	MKK4	1	P45983	JNK1	11062067
O43318	TAK1	1	P46734	MKK3	15837794
P46734	MKK3	1	Q16539	P38	7535770
O43318	TAK1	1	O14920	IKK	11460167
P19438	TNFR	1	P19174	PLC	12645577
P19174	PLC	1	P17252	PKC	12645577
P17252	PKC	1	P12931	SRC	12645577
P12931	SRC	1	O14920	IKK	12645577
P12931	SRC	1	P42336	PI3K	7797556
P12931	SRC	1	P04049	RAF1	7517401
P12931	SRC	1	P29353	SHC	10523831
P29353	SHC	1	P62993	GRB2	10523831

**Table S4. Literature-derived directed network.** Experimental data describing the functional relationships between signaling proteins in the pathways of interest were collected from the literature (Pmid column). This information is represented as a signed directed model, where edges have sign (activating, indicated as 1, or inhibitory, indicated as -1) and directionality (enzyme–substrate relationships). For each protein, Uniprot ID and gene name have been reported.

Phosphatase	Observed phenotype in siRNA screening	Literature experimental evidence	Pmid
PPP3CA	LC3 dots increase	Calcineurin (PPP3CA) defective strains exhibit enhanced autophagy	19279398
MTMR2	rpS6 (P) decrease	MTMR2 over-expression increase AKT activation	19912440
PTPN9	rpS6 (P) increase	PTPN9 inhibition augmented the phosphorylation of AKT in response to insulin	16679294
PPP2R5C	rpS6 (P) increase	PPP2R5C counteracts p70S6K phosphorylation	20444422
PPP2CA	rpS6 (P) increase	Inhibition of PP2A, by okadaic acid, partially reverses inactivation of mTORC1 substrates	20639120
PTPN1	rpS6 (P) increase	PTP-1B <sup>-/-</sup> adipose shows an increased basal activity of p70S6K	17664276
PTPN21	ERK (P) decrease	PTPN21 activates SRC tyrosine kinase and increases the ERK phosphorylation	15143158
DUSP4	p38 (P) decrease	mice DUSP4 <sup>-/-</sup> show a decreased phosphorylation of p38	20351138
PPM1B	NFkB activity increase	Overexpression of PPM1B results in dephosphorylation of IKKbeta and termination of NF-kappaB activation	18930133
PPP2R1A	NFkB activity increase	PPP2R1A binds the CBM complex, inactivating the NFkB signaling	21157432
DUPD1	ERK (P) increase	DUPD1 is a MAPK phosphatase	21199871

**Table S5. Literature reported phosphatase-pathway relationship.** An extensive literature curation was carried out and phosphatase-pathway relationships already described were annotated.

## ■ References

1. Neumann, B. et al. Phenotypic profiling of the human genome by time-lapse microscopy reveals cell division genes. *Nature* **464**, 721-727 (2010).
2. Yuan, J.S., Reed, A., Chen, F. & Stewart, C.N., Jr. Statistical analysis of real-time PCR data. *BMC Bioinformatics* **7**, 85 (2006).